

**HOT COMPRESSION TEST OF 9 Cr-1 Mo STEEL – NUMERICAL SIMULATION**

*Alica Fedoriková<sup>1)\*</sup>, Tibor Kvačkaj<sup>1)</sup>, Róbert Kočíško<sup>1)</sup>, Róbert Bidulský<sup>1)</sup>, Patrik Petroušek<sup>1)</sup>, Jana Bidulská<sup>1)</sup>, Lucia Domovcová<sup>2)</sup>*

*<sup>1)</sup> Institute of Materials, Faculty of Metallurgy, Technical University of Košice, Košice, Slovakia*

*<sup>2)</sup> ZP Research and Development Centre, Podbrezova, Slovakia*

Received: 21.09.2015

Accepted: 08.06.2016

\*Corresponding author: *e-mail: alica.fedorikova@tuke.sk Tel.: +421 55 602 4298, Institute of Materials, Faculty of Metallurgy, Technical University of Košice, Letná 9, 04200 Košice, Slovakia*

**Abstract**

This paper is focused on the evaluation of formability of heat resistant steel type 9Cr-1Mo by laboratory numerical simulation – hot compression test confirmed by laboratory hot compression test. The 9Cr-1Mo steel represents modern 9%Cr tempered martensitic steel for high temperature applications in advanced thermal power plants. Numerical simulations were computed in software Deform 3D for five proposed sample shapes. On the base of normalized Cockcroft-Latham criterion (nCL), indicating the material damage during deformation, the sample type “tapered roller with four axial notches” was found to be the most suitable for hot workability evaluation. On base of simulations, it is also evaluated the temperature range of the workability of 9Cr-1Mo. The interval of good workability according to the nCL criteria is in the temperature range from 650 to 950 °C.

**Keywords:** Finite element analysis, hot pressing, normalized Cockcroft-Latham criterion, austenitic steel: 9Cr-1Mo

**1 Introduction**

The improvement of thermal efficiency by increasing the operating temperature and pressure of boilers has recently led to the development of new grades of creep-resistant steels [1]. Shi et al. [2] showed that modified 9-12% Cr steels improved properties of heat-resistant steels.

The 9Cr-1Mo steel represents tempered martensitic steel with complex alloying assuring transformation, solid solution and precipitation strengthening at elevated temperatures [2]. It is used for thick section components of steam generators operating in the temperature range 550 – 650 C. The presence of precipitated particles formed in the microstructure of 9Cr-1Mo steels during annealing may cause formation of the voids during plastic deformation [3]. This steel grade achieves better mechanical properties with the simultaneous reduction of the wall thickness. Maximum value of creep tensile strength  $R_{m/105h}$  is 110 – 120MPa. The common heat treatment of high Cr steels consists of normalizing and tempering. Because of high Cr content, cooling in air from austenitising temperature leads to fully martensitic microstructure [4]. 9Cr-1Mo steel has been widely applied to manufacture steam containers in ultra-super-critical power plants. The most research focused on 9Cr-1Mo steel investigates microstructure and its behavior during hot deformation, strengthening mechanism and long-term creep properties and corrosion resistance [7-10]. 9Cr-1Mo steel is suitable for welding and there are several impact studies about correlation between microstructure and conditions of welding with others materials and

post-weld heat treatment [11, 12]. Workability and fracture limit criterions have not been determined yet. Because many kind of alloying elements exist in the steel and the microstructure evolution is complicated during hot working, it is difficult to establish the hot working regime [2].

Workability can be defined as the degree of deformation that can be achieved in a particular metalworking process without creating undesirable condition and defects [13]. More recently, a new approach consisting of evaluating, with finite element analysis, the void nucleation, growth and coalescence in a representative cell containing a simple cavity and embedded in a matrix was proposed. This approach has been applied to study ductile damage phenomena for several kinds of loading conditions and to characterize the propensity to cracking. The approach is currently referred to as macroscopic since the scale of the cell lies between the size of the grain (microscopic) and that of the specimen (macroscopic) [14]. Ductile fracture criterions can be used to describe workability of metals. The critical value of stress at which the damage of material appears, the strain and strain rate are the basic parameters describing the limit workability of material. This property depends on the material itself which is being processed but also on the geometry of the specimen and the lubrication conditions.

The simple ductile fracture criterion proposed by Cockcroft and Latham was used for theoretical analysis. This criterion states that fracture occurs when the tensile strain energy reaches a critical value [15], [16]. The Cockcroft-Latham (CL) criterion is described by equation (1):

$$\int_0^{\bar{\varepsilon}} \sigma_1 d\bar{\varepsilon} = C_1 \quad (1.)$$

where  $\sigma_1$  [MPa] – largest principal tensile stress

$\varepsilon$  [-] – strain

$\bar{\varepsilon}_f$  [-] – strain in fracture

$C_1$  [MPa] – material constant – value of the criterion at the instant of fracture initiation

[17].

According to this criterion, if on the material acts only compressive stress, the fracture will not occur. CL criterion does not consider the impact of hydrostatic stress. Oh et al. [18] have modified a CL criterion for uni-axial stress through normalizing of maximum principal tensile stress. This form called a normalized CL criterion (nCL) (2):

$$\int_0^{\bar{\varepsilon}} \frac{\sigma_1}{\bar{\sigma}} d\bar{\varepsilon} = C_2 \quad (2.)$$

where  $\bar{\sigma}$  [MPa] – effective stress

$C_2$  [MPa] – material constant [17].

On the basis of known material constants  $C_1$  or  $C_2$  it can be characterized workability of the material [10]. Using those criteria and values we expect of fracture, but these mathematical simulations should be verified by physical and thus accurately determine their value and terms of workability of the material [17]-[19].

The stress and strain distribution in upsetting deformation represents the typical stress/strain states in most bulk forming processes [15]. Because of this, it was chosen a hot upsetting test.

In **Fig.1** pseudo-binary phase diagram for steel grade 9Cr-1Mo is shown. **Fig. 1** demonstrates that for the 9Cr-1Mo type steel with 0.1 wt. % C, the Ac1 and Ac3 critical transformation temperatures of ferrite to austenite phase transformation are 840 °C and 860 °C, respectively [20].

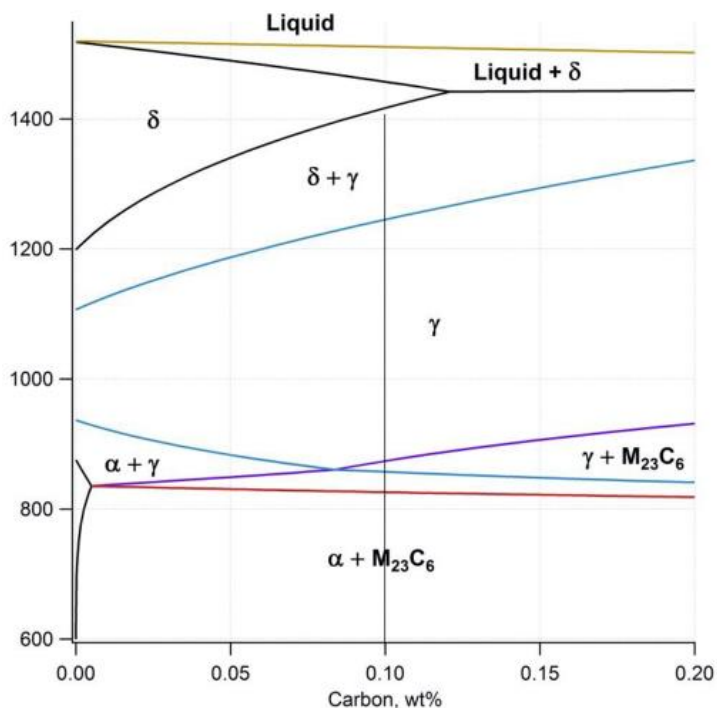


**Fig. 1** Binary phase diagram of steel grade 9Cr-1Mo [20]

This paper is focused on numerical simulations of hot upsetting test of 9Cr-1Mo steel and on selection of the most suitable shape of sample for this test. The suitable temperature range for good workability of studied 9Cr-1Mo steel was evaluated.

## 2 Experimental material and methods

Heat-resistant chromium steel type 9Cr-1Mo was used as experimental material. The chemical composition is given in **Table 1**.

**Table 1** Chemical composition of steel 9Cr-1Mo in wt%

<b>C</b>	<b>Cr</b>	<b>W</b>	<b>Mn</b>	<b>Mo</b>	<b>Si</b>	<b>V</b>	<b>Ni</b>
0.106	8.85	1.864	0.447	0.417	0.298	0.24	0.136
<b>Nb</b>	<b>Cu</b>	<b>Al</b>	<b>Co</b>	<b>P</b>	<b>S</b>	<b>Ti</b>	<b>Fe</b>
0.095	0.07	0.039	0.036	0.018	0.002	<0.003	87.38

Numerical simulations were calculated for this type of material in software Deform 3D. According to [13-15, 21-23] it was designed five types of samples, as it is given at **Fig. 2**.

For every sample type the simulation was performed in isothermal conditions for temperature range from 700 °C to 1100 °C. The setting of each simulation included the same values of maximal strain to be 75 % with an initial strain rate  $\dot{\varphi} = 0,044 \text{ s}^{-1}$ .

Hot compression test was realized with using the last sample type - tapered with four axial notches in the temperature range  $T \in \langle 500; 950 \rangle$ .

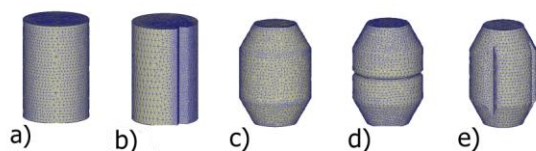


**Fig. 2** The proposed shapes of samples: a) cylindrical, b) cylindrical with one axial notch, c) tapered, d) tapered with one radial notch, e) tapered with four axial notches

### 3 Results

Values of indicator Damage have been monitored which correspond with value of nCL criterion. Color scheme has for every simulation equal interval nCL criteria  $\langle 0; 0,7 \rangle$ . Based on these results it was possible to identify the most probable place origin of cracks and compare value of nCL criterion for individual type of sample.

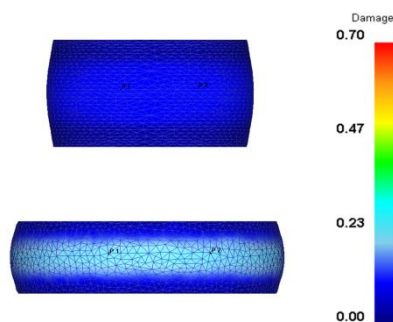


**Fig. 3** Numerical simulation of 50% and 66% deformation – cylindrical sample

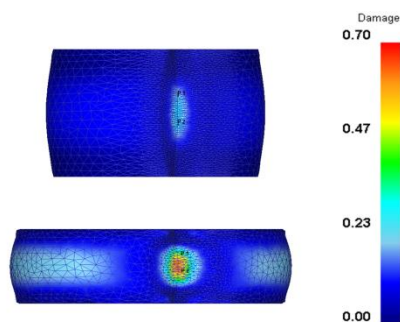


**Fig. 4** Numerical simulation of 50% and 66% deformation – cylindrical sample with one axial notch

In **Fig. 3** cylindrical sample after 50% and 66% deformation at temperature 700°C is shown. Points P1 and P2 have been placed in the area of the highest tensile stress. **Fig. 4** shows cylindrical sample with one axial notch. The highest tensile stress is located in the middle of the notch as it acts like a stress concentrator.

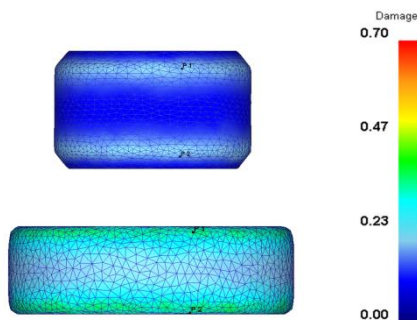


**Fig. 5** Numerical simulation of 50% and 66% deformation – tapered sampl

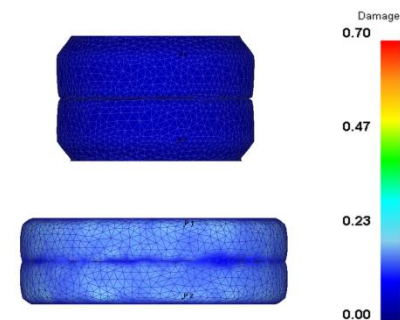


**Fig. 6** Numerical simulation of 50% and 66% deformation – tapered sample with one radial notch

**Fig. 5** shows tapered sample. According to the simulation, it can be assumed that the first was deformed the tapered portions, wider central portion was initially deformed only slightly. After upsetting the tapered portions, deformation of the central part is visible. Deformation is centred on the perimeter at the edge of the tapered and central part. It is seen, that buckling is in this case minimized. In the fields of maximum tensile stress at 66 % strain, the nCL criterion for the simulation of tapered sample shows lower value, compared to that of the cylindrical sample with one axial notch. In **Fig. 6** tapered sample with one radial notch in its central part is shown. Deformation process is similar to the process for tapered sample. Because of small buckling, the notch is pushed into the sample and does not act like a stress concentrator.

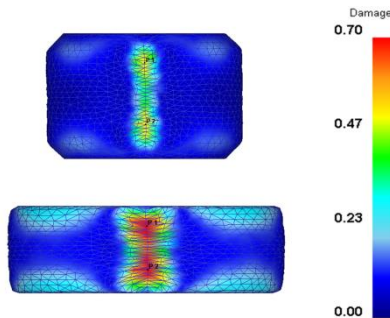


**Fig. 7** Numerical simulation of 50% and 66% deformation – tapered sample with four axial notches

**Fig. 7** shows the deformation of the tapered sample with four axial notches. As in the previous two types of sample, as first the tapered parts are deformed, then the central one. Stress concentration at the edges combined with notches formed in every notch two fields of maximum tensile strength. In these fields in the state of 66% strain has the nCL criterion the highest value compared to the previous shapes of samples.

Values of nCL criterion for all type of samples are shown in **Table 2**.

**Table 2** Maximum values of nCL criterion

Type of sample	nCL [-] $\epsilon = 40\%$	nCL [-] $\epsilon = 50\%$	nCL [-] $\epsilon = 66\%$
Cylindrical	0.067	0.107	0.23
Cylindrical_1x_axial	0.147	0.243	0.646
Tapered	0.147	0.204	0.377
Tapered_1x_radial	0.151	0.194	0.35
Tapered_4x_axial	0.366	0.523	0.739

**Fig. 8** shows nCL value as a function of strain. The curve representing the tapered sample with four axial notches is above the others. It can be concluded that the most appropriate type of sample is tapered with four axial notches and the simple cylindrical sample is the least appropriate for workability evaluation through hot upsetting test. **Fig. 9** depicts the individual sample types with their corresponding nCL values for strain levels of 50 % and 66 %.

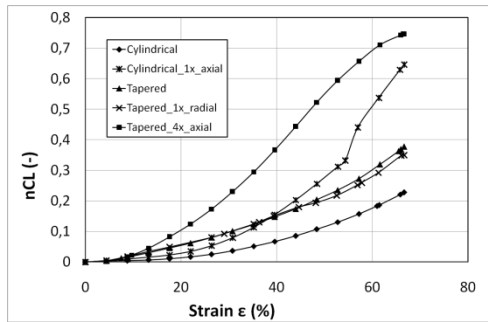


**Fig. 8** Comparison of a  $\varepsilon - nCL$  curves for different types of samples

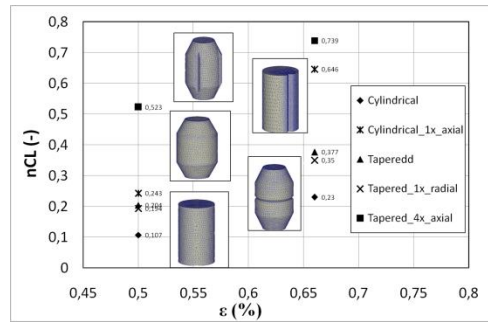


**Fig. 9** nCL dependence for the relative deformation for different types of samples

**Fig. 10** shows that for all sample types except tapered with axial notches has nCL criterion as a function of strain constant progress. The curve representing tapered sample with axial notches is above the others. For strain  $\varepsilon = 50\%$  is the course of function  $nCL - T$  is approximately constant. Only for tapered sample type with axial notches at temperature  $650^\circ\text{C}$  nCL value starts to decrease up to  $900^\circ\text{C}$ , then has the function increasing tendency again, **Fig. 10**. For strain  $\varepsilon = 66\%$  is this decrease more visible. On the basis of significant decrease in nCL value, **Fig. 11** indicates suitable conditions for forming process up to temperature of  $1050^\circ\text{C}$  at the strain level of 66 %.

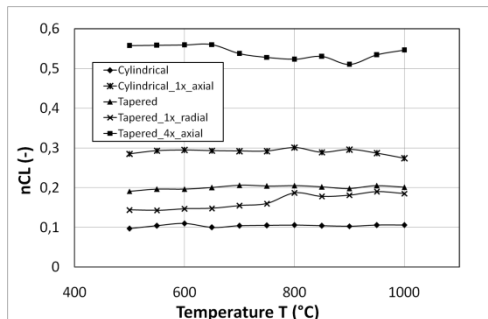


**Fig. 10** nCL values as a function of temperature at strain  $\varepsilon = 50\%$

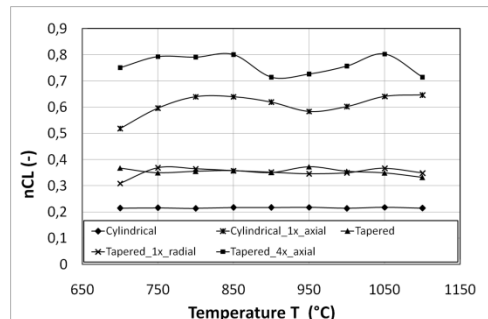


**Fig. 11** nCL values as a function of temperature at strain  $\varepsilon = 66\%$

In **Fig. 12** is a graphical comparison of the course of values nCL criterion dependence on temperature criteria for two types of samples which under previous simulations have been evaluated as the most valuable for hot upsetting test. For the both sample types the values of nCL criterion were evaluated for strain levels of 50 % and 66 %. For the tapered sample with axial notches the nCL value decreased at  $850^\circ\text{C}$  due to the occurrence of ferrite to austenite phase transformation. At  $850^\circ\text{C}$  for tapered sample with axial notches nCL value has been decreased because of phase transition. For cylindrical sample with one axial notch is the decline less pronounced.

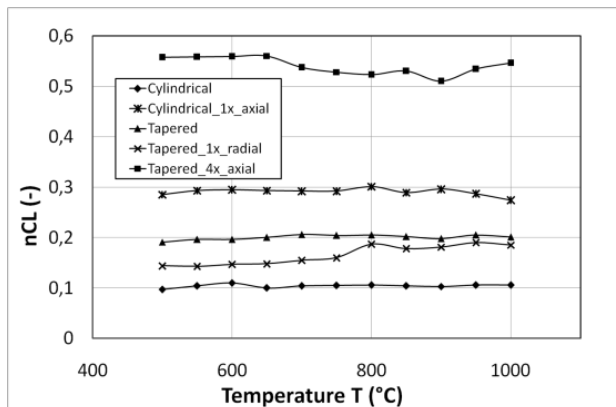


**Fig. 12** Graphical comparison of the nCL criterion as a function of temperature for the most suitable samples for hot workability evaluation

#### 4 Discussion

In evaluating the most appropriate form of samples was used Deform 3D function Point Track, which tracks change the parameter Damage to the time at specified points. These points were determined on the basis of an estimate by the colour scale and have been placed in locations where they operate probably the largest tensile stresses which, above a certain value to cause a fracture. Damage parameter can be evaluated in this case using the distribution of values in the section outlined by the sample, but of the maximum nCL were different order of thousandths. For this reason, it is possible to consider the chosen tool Point Track as sufficient.

The tapered sample with four axial notches has been evaluated as the most suitable form of the sample because of the highest value of the nCL. It is possible to continue to work on the dimensions of sample. Those should be designed according to the requirements of the device, take into account the dimensions of swages and maintain the required ratio between the area of a flat base of swages and the sample.

By physical simulation it is possible to evaluate the workability and compare the results with numerical simulations. According to these the good workability for 9Cr-1Mo steel is at the temperature range 650 -1050°C, depending on the required deformation.

#### 5 Conclusion

The results obtained from numerical simulations of 9Cr-1Mo steel hot compression test can be summarized in the following conclusions:

- According to the nCL values from simulations, the tapered roller with four axial notches was identified as the most suitable sample shape for hot workability evaluation. The cylinder with smooth surface was found to be the least appropriate.
- Depending on the desired deformation, the course of nCL criteria specified by the simulation indicated good workability of studied 9Cr-1Mo steel in the temperature range 650 °C - 1050 °C.

#### References

- [1] J.C. Vaillant, B. Vandenberghe, B. Hahn, H. Heuser, C. Jochum: International Journal of Pressure Vessels and Piping, Vol. 85, 2008, No. 1-2, p. 38-46, DOI:10.1016/j.ijpvp.2007.06.011

- [2] R. Shi, Z. Liu: *Journal of Iron and Steel Research, International*, Vol. 18, 2011, No. 7, p. 53-58, DOI:10.1016/S1006-706X(11)60090-3
- [3] J. Blach, L. Falat, P. Švec: *Engineering Failure Analysis*, Vol. 16, 2009, No. 5, p.1397-1403, DOI: 10.1016/j.engfailanal.2008.09.003
- [4] L. Falat, A. Výrostková, V. Homolová, M. Svoboda: *Engineering Failure Analysis*, Vol. 16, 2009, No. 7, p.2114-2120, DOI: 10.1016/j.engfailanal.2009.02.004
- [5] V. Sklenička, K. Kuchařová, M. Svoboda, L. Kloc, J. Buršík, A. Kroupa.: *Materials Characterization*, Vol. 51, 2003, No.1, p. 35-48, DOI:10.1016/j.matchar.2003.09.012
- [6] V. Sklenička, K. Kuchařová, P. Král, M. Kvapilová, M. Svobodová, J. Čmakal: *Materials Science and Engineering A*, Vol. 644, 2007, p. 297-309, DOI: 10.1016/j.msea.2015.07.072
- [7] P.J. Ennis, A. Zielinska-Lipiec, O. Wachter, A. Czyska-Filemonowicz: *ActaMaterialia*, Vol. 45, 1997, No. 12, p. 4901-4907, DOI:10.1016/S1359-6454(97)00176-6
- [8] V.A. Yardley, T. Matsuzaki, R. Sugiura, A.T. Yokobori Jr., S. Tsurekawa, Y. Hasegawa: *Journal of Physics: Conference Series*, Vol. 240, 2010, No. 1, DOI: 10.1088/1742-6596/240/1/012076
- [9] N.Q. Zhang, H. Xu, B.R. Li, Y. Bai, D.Y. Liu: *Corrosion science*, Vol. 56, 2012, p. 123-128, DOI: 10.1016/j.corsci.2011.11.013
- [10] L. Tan, X. Ren, T.R. Allen: *Corrosion science*, Vol.52, 2010, No. 4, p. 1520-1528, DOI: 10.1016/j.corsci.2009.12.032
- [11] L. Falat, L. Čiripová, J. Kepič, J. Buršík, I. Podstranská: *Engineering Failure Analysis*, Vol. 40, 2014, p. 141-152, DOI: 10.1016/j.engfailanal.2014.02.018
- [12] L. Falat, A. Výrostková, M. Svoboda, O. Milkovič: *Kovovematerialy*, Vol. 49, 2011, No. 6, p. 417-426, DOI: 10.4149/km-2011-6-417
- [13] B.P.P.A. Gouveia, J.M.C. Rodrigues, P.A.F Martins: *International Journal of Mechanical Sciences*, Vol. 38, 1996, p. 361-372. DOI: 10.1016/0020-7403(95)00069-0
- [14] J. Ladre, et al.: *Finite elements in Analysis and Design*, Vol. 39, 2003, No. 3, p. 175-186: DOI:10.1016/S0168-874X(02)00065-3
- [15] H. Li, M.W. Fu, J. Lu: H. Yang: *International Journal of Plasticity*, Vol. 27, 2011, No. 2, p. 147-180, DOI: 10.1016/j.ijplas.2010.04.001
- [16] M.G. Cockroft, D.J. Latham: *Journal of Institute of Metals*, Vol. 96, 1968, p.33-39
- [17] T. Kvačkaj, R. Kočiško, J. Tiža, J. Bidulská, A. Kováčová, R. Bidulský, J. Bacsó, M. Vlado: *Archives of Metallurgy and Materials*, Vol. 58, 2013, No. 2, p. 407-412, DOI: 0.2478/amm-2013-0008
- [18] S.I. Oh, C.C. Chen, S. Kobayashi: *Journal of Engineering for Industry – Transactions of the ASME*, Vol. 101, 1979, p. 36-44, DOI: 10.1115/1.3439471
- [19] C.C. Huang, J.H. Cheng: *International Journal of Mechanical Sciences*, Vol. 45, 2005, No. 7, p. 1123-1145, DOI: 10.1016/j.ijmecsci.2005.02.014
- [20] Y. Yamamoto, M. Santanela, S. Babu, X. Yu: *Improving the Performance of Creep-Strength-Enhanced Ferritic (CSEF) Steels*, In: 26th Annual Conference on Fossil Energy Materials, Pittsburgh, PA, US Department of Energy, Office of Fossil Energy 2012, [1.5.2015], <https://www.netl.doe.gov/File%20Library/Events/2009/fem/Santella.pdf>
- [21] P. Petroušek et al.: *Acta Metallurgica Slovaca*, Vol. 21, 2015, No. 3, p. 176-183, DOI: 10.12776/ams.v21i3.615
- [22] R. Kočiško, R. Bidulský, L. Dragošek, M. Škrobjan: *Acta Metallurgica Slovaca*, Vol. 20, 2014, No. 3, p. 302-308, DOI: 10.12776/ams.v20i3.366

[23] L. Dragošek, R. Kočiško, A. Kováčová, R. Bidulský, M. Škrobán: Acta Polytechnica, Vol. 55, 2015, No. 5, p. 301-305, DOI: 10.14311/AP.2015.55.0301

### **Acknowledgement**

*This work was realized within the frame of the Operational Program “Research and Development” „Centre of research of efficient integration of combined systems based on renewable energy sources“ project ITMS 26220220064 and financially supported by a European Regional Development Fund.*